LETTER TO THE EDITOR

Allograft inflammatory factor-1 is essential for acute monocytic leukemia infiltration

Authors

Ai-Li Chen,[1-4*] Hai-Yang Hu,[2-4*°] Doaa Alamoudi,[2-4°] Jia-Yang Zhang,[5,6] Shi-Jie Yao,[2-4°] Bi-Huan Zhao,[7] He-Yu Song,[7] Hong-Hu Zhu[5,7] and Qian-Fei Wang[2-4]

[1]Medical Research Center, Beijing Chao-Yang Hospital, Capital Medical University; [2]China National Center for Bioinformation; [3]Beijing Institute of Genomics, Chinese Academy of Sciences; [4]University of Chinese Academy of Sciences; [5]Department of Hematology, Beijing Chao-Yang Hospital, Capital Medical University; [6]The Postgraduate Training Base of Jinzhou Medical University (The PLA Rocket Force Characteristic Medical Center) and [7]Chinese Institute for Medical Research, Capital Medical University, Beijing, China

**ALC and HYH contributed equally as first authors.*

°Current address
HYH: Beijing An Zhen Hospital, Capital Medical University, Beijing, and Beijing Institute of Heart, Lung and Blood Vessel Diseases, Beijing, China
DA: Genomic Medicine Center of Excellence, King Faisal Specialist Hospital & Research Centre, Riyadh, Saudi Arabia
SJY: Department of Cell Biology, School of Basic Medical Sciences, Peking University Health Science Center, Peking University, Beijing, China

Correspondence:
AI-LI CHEN - chenal@mail.ccmu.edu.cn
QIAN-FEI WANG - wangqf@big.ac.cn

https://doi.org/10.3324/haematol.2025.300027

Received: October 11, 2025.
Accepted: April 17, 2026.
Early view: April 23, 2026.

©2026 Ferrata Storti Foundation
Published under a CC BY-NC license

Supplementary Figure Legends:

Supplementary Figure S1. AIF1 expression and prognosis in various public cohort.

A. The differences in adhesion and migration characteristics between FAB subtypes M4/M5 and other FAB subtypes by GSEA in TCGA, TARGET, GSE1159 and GSE6891 public cohorts.
B. Overlap of genes associated with cell infiltration, specifically highly expressed in the hematopoietic system, and upregulated in M4/M5 subtypes compared to other AML subtypes across four independent datasets.
C. Predicted interaction relationships among the eight overlapping genes by Signaling Network Integrated Analysis Platform (STRING).
D. Distribution of *AIF1* expression in neutrophil/monocyte and non-neutrophil/monocyte cells from healthy donors or AML patients at diagnosis, along with a ridge plot of the expression of *AIF1* in different cell types from AML patients at diagnosis in scRNA-seq data.
E. The expression of *AIF1* in different AML FAB subtypes, healthy individuals (N= 8) vs CD14 top quartile AML patient blasts (N=70) in the GSE1159.
F. The expression of *AIF1* in different AML FAB subtypes, *AIF1* healthy individuals (N= 19) vs CD14 top quartile AML patient blasts (N=76) in the Beat AML.
G. The expression of *AIF1* in different AML FAB subtypes and risk groups in the GSE14468.
H. Kaplan-Meier curves showing the event-free survival (EFS) and overall survival (OS) of TARGET-AML patients stratified by the median expression of *AIF1*.
I. Kaplan-Meier curves showing the event-free survival (EFS) and overall survival (OS) of TARGET M4&M5 AML patients stratified by the median expression of *AIF1*.
J. Univariate Cox regression analysis was performed to evaluate the prognostic impact of *AIF1* expression on event-free survival (EFS) and overall survival (OS) in three independent cohorts (TCGA, TARGET, and GSE37642). Based on AIF1 expression levels, patients were divided into high- and low-expression groups using the best cutoff determined by the survminer R package. This analysis was applied to the overall cohort as well as to the M1, M2, M4, and M5 FAB subtypes. Hazard ratios (HRs) with 95% confidence intervals (CIs) and p-values were calculated to assess the risk associated with higher *AIF1* expression.

Statistical significance: *p<0.05, **p<0.01, ***p<0.001;
Comparisons: * vs. mean expression level of *AIF1* (Anova test).

Supplementary Figure S2. AIF1 is essential for AMoL growth and infiltration.

Monocytic and non-monocytic cell lines were transduced with scramble control (shCon) and *AIF1* shRNA (sh*AIF1*-1/2) by lentivirus. RNA was extracted 48 hours after sorting,

and *AIF1* expression levels were assessed using real-time quantitative PCR. Relative *AIF1* expression of each sample was normalized to its GAPDH expression and then compared with shCon.

A. Relative *AIF1* expression and growth curves of monocytic cell lines U937 and MV4-11 following *AIF1* knockdown.
B. Relative *AIF1* expression and growth curves of non-monocytic cell lines Kasumi and K562 following *AIF1* knockdown.
C. Left panel: Cell apoptosis of THP-1 cells transduced with shCon or sh*AIF1*, assessed by flow cytometry, stained by Annexin-V and 7AAD. Right panel: Cell cycle change of THP-1, U937 and MV4-11 cells transduced with shCon or sh*AIF1*, assessed by flow cytometry, stained by PI.
D. Migration or invasion assay of U937 or THP-1 cells transduced with shCon, sh*AIF1* and/or *AIF1*. For invasion assay, Transwell inserts were coated with Matrigel. Cells were serum-starved for 20 hours, then seeded into the upper chamber. The lower chamber contained RPMI 1640 medium with 20% FBS. After 5 hours of incubation at 37°C with 5% CO_2, cells infiltrated to the lower chamber were counted to calculate the invasion ratio.
E. Relative *AIF1* expression and migration assay of non-monocytic cell line Kasumi-1 following *AIF1* overexpression. Left panel: Relative *AIF1* expression normalized to its GAPDH expression. Right panel: Migration ratio of Kasumi-1 cells transduced with *AIF1*. Cells migrated to the lower chamber are counted to calculate migration ratio.
F. Adhesion assay of THP-1 and U937 cells transduced with shCon or sh*AIF1* to MS-5 mouse bone marrow stromal cells. Cells were co-cultured for 1h, and washed with medium twice, the rest of cells were quantified to calculate the adhesion ratio of THP-1 to MS-5 cells.
G. Infiltration of *AIF1*-knockdown THP-1 cells (mCherry-positive cells) in the bone marrow, liver, and kidneys of NSG mice after transplantation.

Statistical significance: *p<0.05, **p<0.01, ***p<0.001;
Comparisons: * vs. shCon，# vs. +*AIF1*, $ vs. sh*AIF1*-1, & vs. sh*AIF1*-2 (t-test).

Supplementary Figure S3. *AIF1* knockdown down-regulated expression of CCR2 while *AIF1* overexpression didn't affect CCR2 expression.

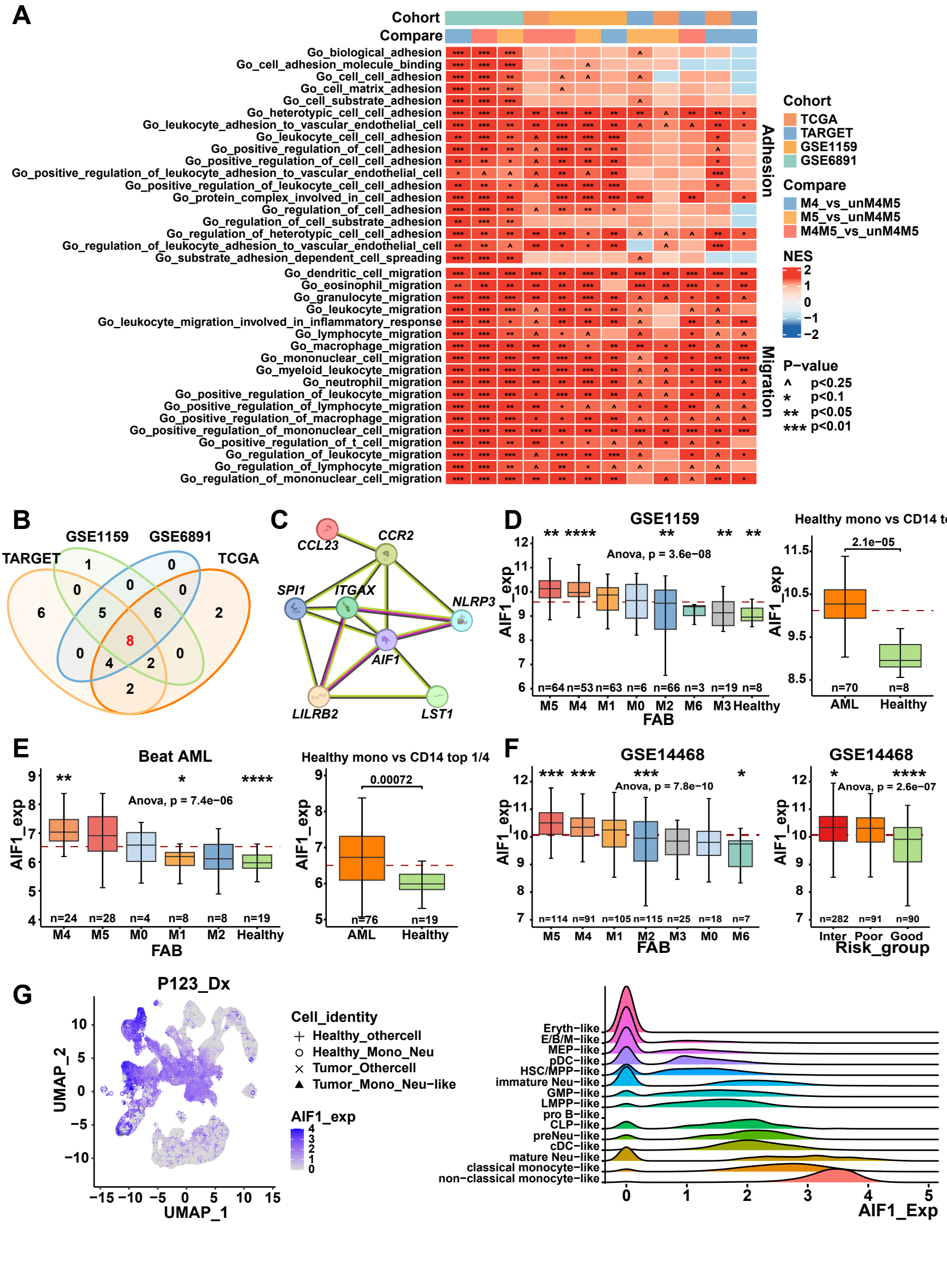
A. Pathway enrichment analysis using Metascape for genes that are consistently downregulated/upregulated under all four conditions (2 cell lines, 2 shRNA) and significantly downregulated in at least two conditions (p<0.05).
B. CCR2 expression on the cell surfaces of THP-1 cells (knockdown or overexpress *AIF1*). Right panel: Mean Fluorescence Intensity (MFI) of CCR2 on the surface of THP-1 cells measured by flow cytometry in three independent experiments.

C. Endogenous CCR2 expression in THP-1 cells transduced with shCon or sh*AIF1* and/or *AIF1*. Relative CCR2 expression of each sample was normalized to its GAPDH expression and then compared with shCon.
D. CCR2 expression on the cell surfaces of U937 cells (knockdown or overexpress *AIF1*). Right panel: Mean Fluorescence Intensity (MFI) of CCR2 on the surface of U937 cells measured by flow cytometry in three independent experiments.
E. Endogenous CCR2 expression of U937 cells transduced with shCon or sh*AIF1*.
F. Downregulation of CCR2 in bulk RNA sequencing after sh*AIF1*-1 and sh*AIF1*-2 knockdown compared to the empty control.
G. Expression of CCR2 in different FAB subtypes in the TCGA cohort, showing a strong positive correlation with *AIF1* expression.

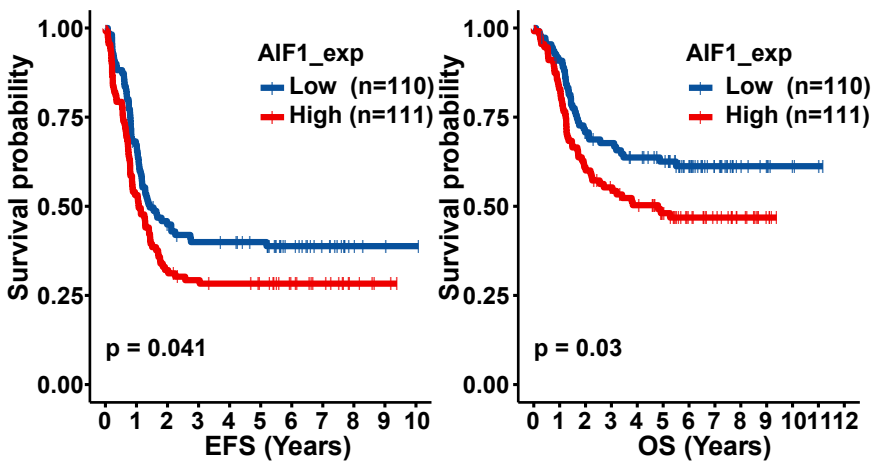
Statistical significance: *p<0.05, **p<0.01, ***p<0.001;

Comparisons: * vs. shCon (t-test) or mean expression level of *AIF1* (Anova test), # vs. +*AIF1* (t-test).

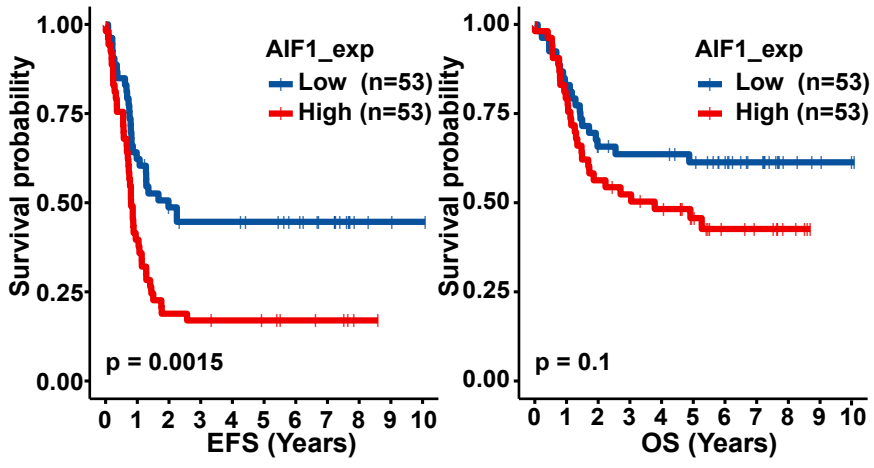
Figure_S1


A
Cohort
Compare
Go_biological_adhesion
Go_cell_adhesion_molecule_binding
Go_cell_cell_adhesion
Go_cell_matrix_adhesion
Go_cell_substrate_adhesion
Go_heterotypic_cell_cell_adhesion
Go_leukocyte_adhesion_to_vascular_endothelial_cell
Go_leukocyte_cell_cell_adhesion
Go_positive_regulation_of_cell_adhesion
Go_positive_regulation_of_cell_cell_adhesion
Go_positive_regulation_of_leukocyte_adhesion_to_vascular_endothelial_cell
Go_positive_regulation_of_leukocyte_cell_cell_adhesion
Go_protein_complex_involved_in_cell_adhesion
Go_regulation_of_cell_adhesion
Go_regulation_of_cell_substrate_adhesion
Go_regulation_of_heterotypic_cell_cell_adhesion
Go_regulation_of_leukocyte_adhesion_to_vascular_endothelial_cell
Go_substrate_adhesion_dependent_cell_spreading
Adhesion
Go_dendritic_cell_migration
Go_eosinophil_migration
Go_granulocyte_migration
Go_leukocyte_migration
Go_leukocyte_migration_involved_in_inflammatory_response
Go_lymphocyte_migration
Go_macrophage_migration
Go_mononuclear_cell_migration
Go_myeloid_leukocyte_migration
Go_neutrophil_migration
Go_positive_regulation_of_leukocyte_migration
Go_positive_regulation_of_lymphocyte_migration
Go_positive_regulation_of_macrophage_migration
Go_positive_regulation_of_mononuclear_cell_migration
Go_positive_regulation_of_t_cell_migration
Go_regulation_of_leukocyte_migration
Go_regulation_of_lymphocyte_migration
Go_regulation_of_mononuclear_cell_migration
Migration
Cohort
TCGA
TARGET
GSE1159
GSE6891
Compare
M4_vs_unM4M5
M5_vs_unM4M5
M4M5_vs_unM4M5
NES
2
1
0
−1
−2
P−value
^ p<0.25
* p<0.1
** p<0.05
*** p<0.01
B
GSE1159
GSE6891
TARGET
TCGA
C
CCL23
CCR2
SPI1
ITGAX
NLRP3
AIF1
LILRB2
LST1
D
GSE1159
Anova, p = 3.6e−08
AIF1_exp
n=64 n=53 n=63 n=6 n=66 n=3 n=19 n=8
M5 M4 M1 M0 M2 M6 M3 Healthy
FAB
Healthy mono vs CD14 top 1/4
2.1e−05
n=70 n=8
AML Healthy
E
Beat AML
Anova, p = 7.4e−06
n=24 n=28 n=4 n=8 n=8 n=19
M4 M5 M0 M1 M2 Healthy
FAB
Healthy mono vs CD14 top 1/4
0.00072
n=76 n=19
AML Healthy
F
GSE14468
Anova, p = 7.8e−10
n=114 n=91 n=105 n=115 n=25 n=18 n=7
M5 M4 M1 M2 M3 M0 M6
FAB
GSE14468
Anova, p = 2.6e−07
n=282 n=91 n=90
Inter Poor Good
Risk_group
G
P123_Dx
UMAP_1
UMAP_2
Cell_identity
Healthy_othercell
Healthy_Mono_Neu
Tumor_Othercell
Tumor_Mono_Neu−like
AIF1_exp
Eryth−like
E/B/M−like
MEP−like
pDC−like
HSC/MPP−like
immature Neu−like
GMP−like
LMPP−like
pro B−like
CLP−like
preNeu−like
cDC−like
mature Neu−like
classical monocyte−like
non−classical monocyte−like
AIF1_Exp

H



I



J

	Whole cohort					
	EFS			OS		
	HR	P_value	95CI	HR	P_value	95CI
GSE37642	--	--	--	1.316	0.019	[1.047,1.654]
Target	1.671	0.002	[1.205,2.315]	1.699	0.009	[1.14,2.531]
TCGA	1.665	0.008	[1.14,2.432]	1.934	0.002	[1.281,2.921]

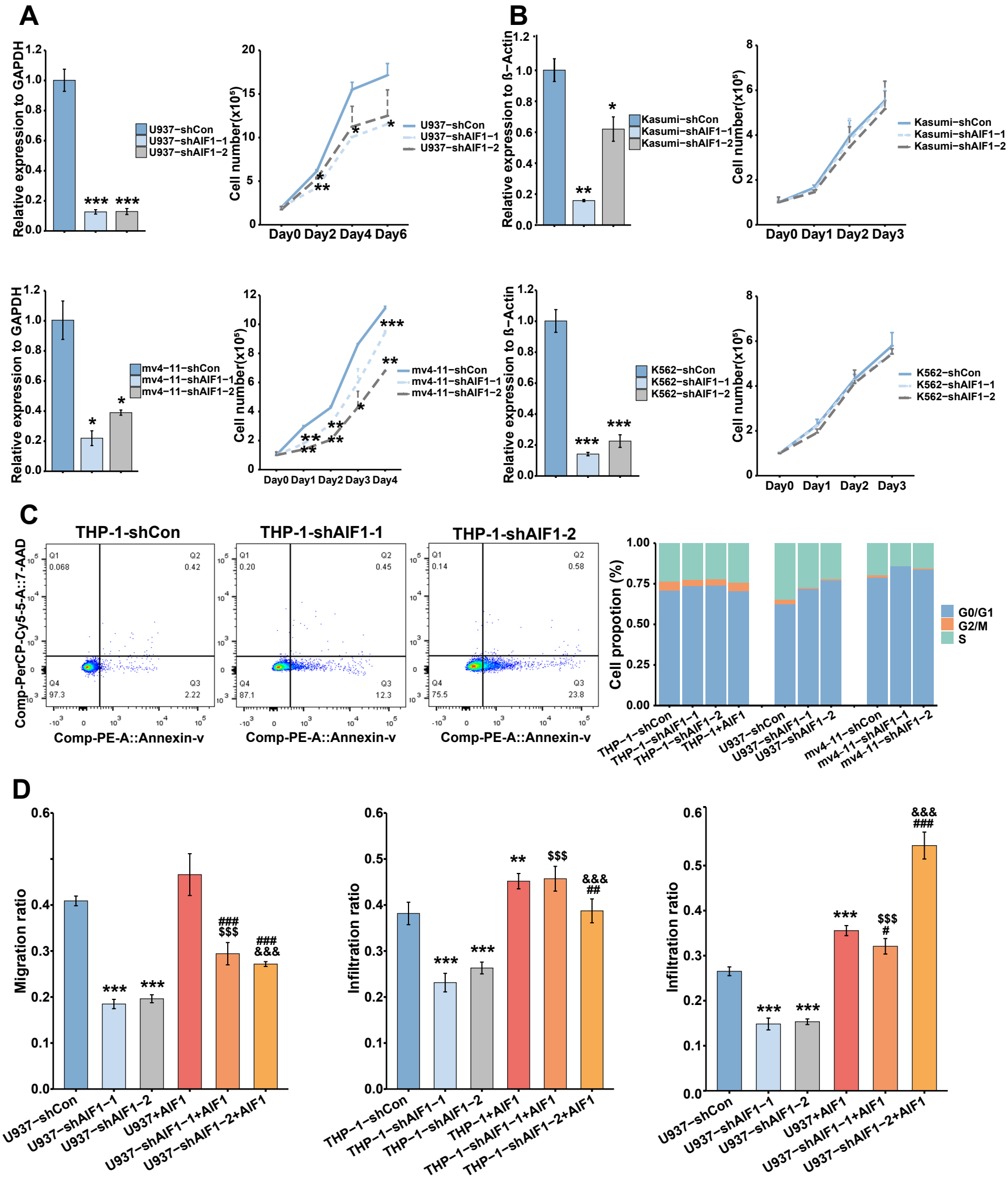
	M1					
	EFS			OS		
	HR	P_value	95CI	HR	P_value	95CI
GSE37642	--	--	--	2.093	0.005	[1.255,3.49]
Target	1.852	0.171	[0.766,4.476]	5.246	0.013	[1.416,19.436]
TCGA	0.844	0.763	[0.28,2.543]	0.629	0.465	[0.182,2.178]

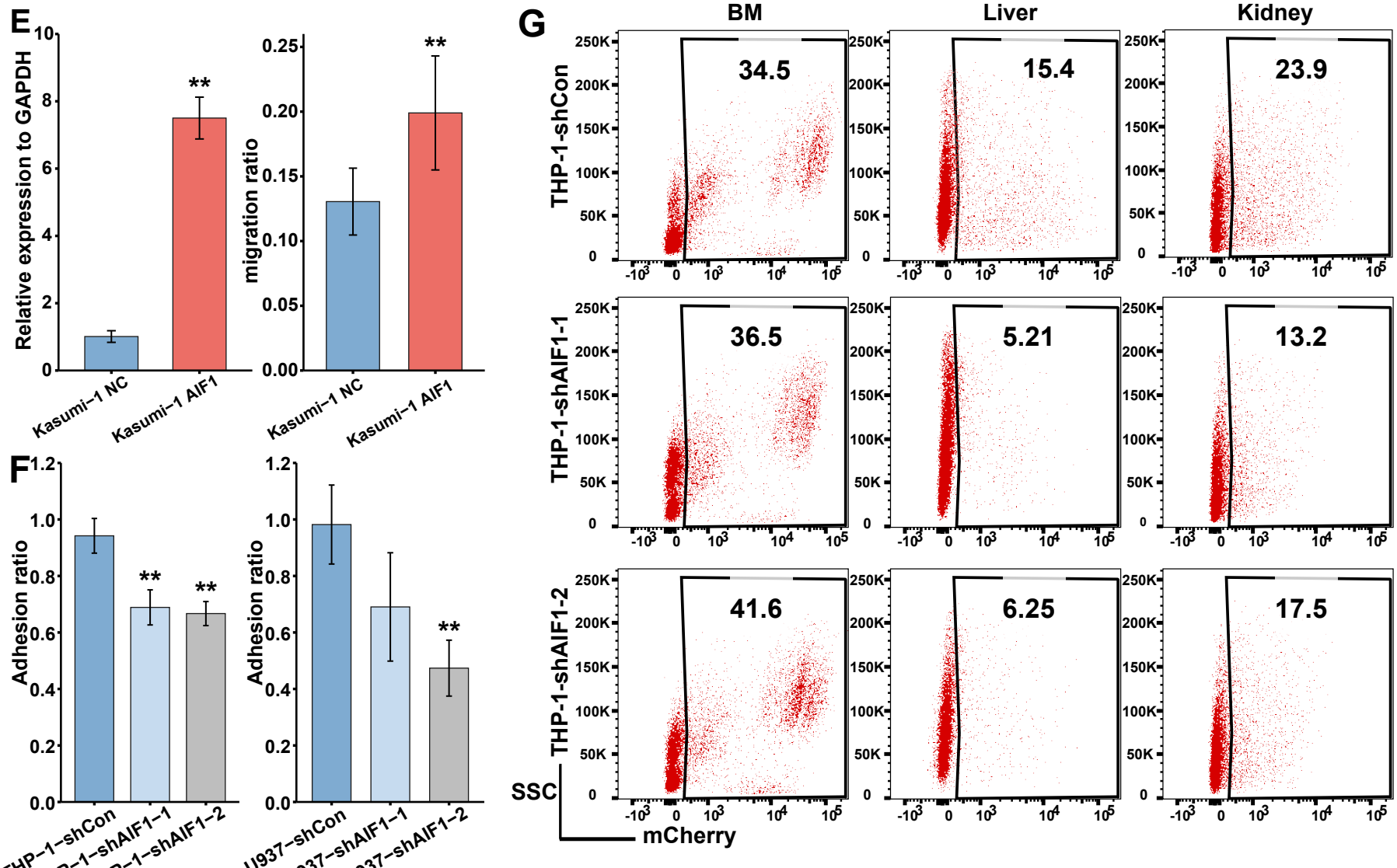
	M2					
	EFS			OS		
	HR	P_value	95CI	HR	P_value	95CI
GSE37642	--	--	--	1.717	0.02	[1.09,2.706]
Target	1.844	0.17	[0.77,4.417]	2.785	0.096	[0.835,9.293]
TCGA	2.801	0.015	[1.225,6.405]	2.931	0.023	[1.158,7.418]

	M4					
	EFS			OS		
	HR	P_value	95CI	HR	P_value	95CI
GSE37642	--	--	--	0.858	0.688	[0.406,1.813]
Target	2.218	0.015	[1.168,4.211]	2.767	0.017	[1.195,6.403]
TCGA	0.883	0.805	[0.328,2.375]	1.321	0.592	[0.477,3.659]

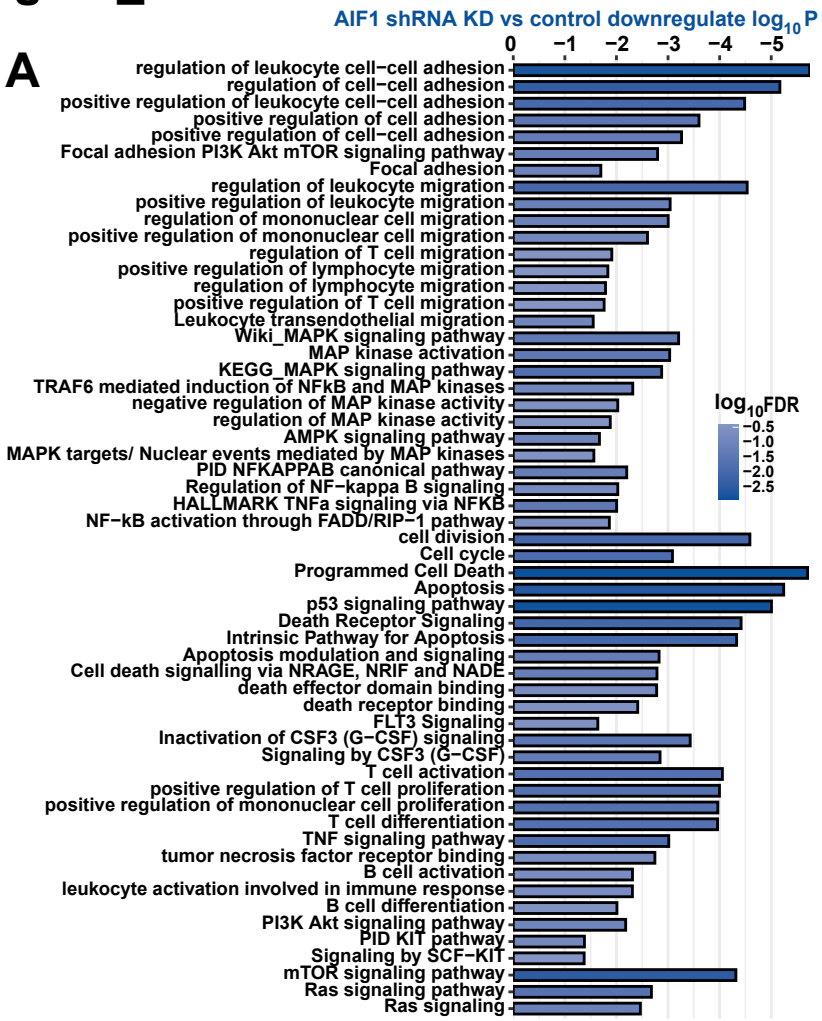
	M5					
	EFS			OS		
	HR	P_value	95CI	HR	P_value	95CI
GSE37642	--	--	--	0.443	0.128	[0.155,1.264]
Target	2.204	0.08	[0.911,5.332]	1.671	0.303	[0.629,4.44]
TCGA	0.42	0.186	[0.116,1.52]	0.395	0.155	[0.11,1.421]

Figure_S2


A
Relative expression to GAPDH
U937−shCon
U937−shAIF1−1
U937−shAIF1−2
Cell number(x10⁵)
Day0 Day2 Day4 Day6
B
Relative expression to ß−Actin
Kasumi−shCon
Kasumi−shAIF1−1
Kasumi−shAIF1−2
Day0 Day1 Day2 Day3
mv4−11−shCon
mv4−11−shAIF1−1
mv4−11−shAIF1−2
Day0 Day1 Day2 Day3 Day4
K562−shCon
K562−shAIF1−1
K562−shAIF1−2
C
THP-1-shCon
THP-1-shAIF1-1
THP-1-shAIF1-2
Comp-PerCP-Cy5-5-A::7-AAD
Comp-PE-A::Annexin-v
Q1 0.068
Q2 0.42
Q4 97.3
Q3 2.22
Q1 0.20
Q2 0.45
Q4 87.1
Q3 12.3
Q1 0.14
Q2 0.58
Q4 75.5
Q3 23.8
Cell propotion (%)
G0/G1
G2/M
S
THP−1−shCon
THP−1−shAIF1−1
THP−1−shAIF1−2
THP−1+AIF1
U937−shCon
U937−shAIF1−1
U937−shAIF1−2
mv4−11−shCon
mv4−11−shAIF1−1
mv4−11−shAIF1−2
D
Migration ratio
U937−shCon
U937−shAIF1−1
U937−shAIF1−2
U937+AIF1
U937−shAIF1−1+AIF1
U937−shAIF1−2+AIF1
Infiltration ratio
THP−1−shCon
THP−1−shAIF1−1
THP−1−shAIF1−2
THP−1+AIF1
THP−1−shAIF1−1+AIF1
THP−1−shAIF1−2+AIF1


E
Relative expression to GAPDH
Kasumi−1 NC
Kasumi−1 AIF1
migration ratio
Kasumi−1 NC
Kasumi−1 AIF1
F
Adhesion ratio
THP−1−shCon
THP−1−shAIF1−1
THP−1−shAIF1−2
Adhesion ratio
U937−shCon
U937−shAIF1−1
U937−shAIF1−2
G
BM
Liver
Kidney
THP-1-shCon
THP-1-shAIF1-1
THP-1-shAIF1-2
34.5
15.4
23.9
36.5
5.21
13.2
41.6
6.25
17.5
SSC
mCherry

Figure_S3


A
AIF1 shRNA KD vs control downregulate log10 P
0 −1 −2 −3 −4 −5
regulation of leukocyte cell−cell adhesion
regulation of cell−cell adhesion
positive regulation of leukocyte cell−cell adhesion
positive regulation of cell adhesion
positive regulation of cell−cell adhesion
Focal adhesion PI3K Akt mTOR signaling pathway
Focal adhesion
regulation of leukocyte migration
positive regulation of leukocyte migration
regulation of mononuclear cell migration
positive regulation of mononuclear cell migration
regulation of T cell migration
positive regulation of lymphocyte migration
regulation of lymphocyte migration
positive regulation of T cell migration
Leukocyte transendothelial migration
Wiki_MAPK signaling pathway
MAP kinase activation
KEGG_MAPK signaling pathway
TRAF6 mediated induction of NFkB and MAP kinases
negative regulation of MAP kinase activity
regulation of MAP kinase activity
AMPK signaling pathway
MAPK targets/ Nuclear events mediated by MAP kinases
PID NFKAPPAB canonical pathway
Regulation of NF−kappa B signaling
HALLMARK TNFa signaling via NFKB
NF−kB activation through FADD/RIP−1 pathway
cell division
Cell cycle
Programmed Cell Death
Apoptosis
p53 signaling pathway
Death Receptor Signaling
Intrinsic Pathway for Apoptosis
Apoptosis modulation and signaling
Cell death signalling via NRAGE, NRIF and NADE
death effector domain binding
death receptor binding
FLT3 Signaling
Inactivation of CSF3 (G−CSF) signaling
Signaling by CSF3 (G−CSF)
T cell activation
positive regulation of T cell proliferation
positive regulation of mononuclear cell proliferation
T cell differentiation
TNF signaling pathway
tumor necrosis factor receptor binding
B cell activation
leukocyte activation involved in immune response
B cell differentiation
PI3K Akt signaling pathway
PID KIT pathway
Signaling by SCF−KIT
mTOR signaling pathway
Ras signaling pathway
Ras signaling
log10FDR
−0.5
−1.0
−1.5
−2.0
−2.5
AIF1 shRNA KD vs control upregulate log10 P
0 −2 −4 −6 −8 −10
intracellular protein transport
protein localization to endoplasmic reticulum
establishment of protein localization to membrane
protein localization to membrane
protein localization to organelle
protein targeting to membrane
establishment of protein localization to endoplasmic reticulum
protein targeting to ER
establishment of protein localization to organelle
post−translational protein targeting to ERM
post−translational protein targeting to membrane, translocation
cotranslational protein targeting to membrane
SRP−dependent cotranslational protein targeting to membrane
intracellular protein transmembrane transport
mRNA Splicing
mRNA Splicing − Major Pathway
Processing of Capped Intron−Containing Pre−mRNA
RNA splicing, via transesterification reactions
mRNA splicing, via spliceosome
mRNA processing
mRNA metabolic process
Unfolded Protein Response (UPR)
response to unfolded protein
proteasomal protein catabolic process
response to topologically incorrect protein
proteolysis involved in protein catabolic process
cellular response to unfolded protein
cellular response to topologically incorrect protein
endoplasmic reticulum unfolded protein response
Adaptive Immune System
Neutrophil degranulation
Antigen processing−Cross presentation
Class I MHC mediated antigen processing & presentation
Folding, assembly and peptide loading of class I MHC
Cytokine Signaling in Immune system
antigen processing and presentation of peptide antigen
MHC class II antigen presentation
antigen processing and presentation of exogenous antigen
cellular respiration
oxidative phosphorylation
electron transport chain
energy derivation by oxidation of organic compounds
aerobic electron transport chain
proton motive force−driven mitochondrial ATP synthesis
ATP synthesis coupled electron transport
mitochondrial ATP synthesis coupled electron transport
mitochondrial electron transport, NADH to ubiquinone
proton motive force−driven ATP synthesis
NADH dehydrogenase complex assembly
mitochondrial respiratory chain complex I assembly
log10FDR
−2
−4
−6
B
THP-1-AIF1
THP-1-Con
THP-1-shAIF1-2
THP-1-shAIF1-1
THP-1-shCon
-10^3 0 10^3 10^4 10^5
Comp-APC-A::CCR2
Mean MFI of APC
0.17
0.103
0.07
THP1−1−shCon
THP−1−shAIF1−1
THP−1−shAIF1−2
THP−1+Con
THP−1+AIF1
C
Relative expression to GAPDH
**
**
###
##
THP−1−shCon
THP−1−shAIF1−1
THP−1−shAIF1−2
THP−1+AIF1
THP−1−shAIF1−1+AIF1
THP−1−shAIF1−2+AIF1
D
U937-AIF1
U937-Con
U937-shAIF1-2
U937-shAIF1-1
U937-shCon
-10^3 0 10^3 10^4 10^5
Comp-APC-A::CCR2
Mean MFI of APC
0.126
0.131
0.186
U937−shCon
U937−shAIF1−1
U937−shAIF1−2
U937+Con
U937+AIF1
E
Relative expression to GAPDH
***
**
U937−shCon
U937−shAIF1−1
U937−shAIF1−2
F
CCR2_exp log (TPM+1)
0.01
0.004
THP−1−shCon
THP−1−shAIF1−1
THP−1−shAIF1−2
0.18
0.18
U937−shCon
U937−shAIF1−1
U937−shAIF1−2
G
TCGA
*
****
****
Anova, p = 3.2e−10
CCR2_exp
n=15 n=29 n=35 n=38 n=15 n=2 n=14
M5 M4 M1 M2 M0 M6 M3
FAB
TCGA
R=0.27p=8e−04
CCR2_exp
AIF1_exp